Journal of Alloys and Compounds, *177* (1991) 83–91
JAL 0071

Proton nuclear magnetic resonance line narrowing and tetragonal lattice distortion in SmH_{2+x} ($0 \leqslant x \leqslant 0.40$)

O. J. Żogał
Institute for Low Temperature and Structure Research, Polish Academy of Sciences, P.O. Box 937, 50-950 Wrocław (Poland)

Ph. l'Héritier
INPG, URA 1109 CNRS, ENS de Physique de Grenoble, B.P. 46, 38402 St. Martin d'Hères Cedex (France)

(Received April 30, 1991; in final form July 3, 1991)

Abstract

Proton magnetic resonance experiments have been made on samarium hydride samples SmH_{2+x} ($0 \leqslant x \leqslant 0.40$) to search for proton self-diffusion and hydrogen ordering effects. Data are presented for the linewidths and some line shapes for temperatures from about 78 K to 295 K. For all samples except $SmH_{2.00}$, proton line narrowing was observed. However, for $x = 0.30$ and $x = 0.40$ a system of two lines appeared below about 250 K. One of these lines is broad, and its second and fourth moments exhibit a weak temperature dependence. This indicates a possible hydrogen sublattice ordering below 250 K since this effect may hinder the proton diffusion and thus a broad resonance line results. Our X-ray studies revealed a very small ($c:a \approx 1.003$) tetragonal deformation in $SmH_{2.30}$ at low temperatures. The effect was much less distinct in $SmH_{2.40}$ and not detected in $SmH_{2.12}$.

1. Introduction

As in the lanthanum hydrides, samarium forms a nonstoichiometric dihydride phase, SmH_{2+x}, over a wide composition range. At room temperature it has the CaF_2-type structure and a continuous solid solution extends from $x \approx -0.05$ to $x \approx 0.34$ [1]. However, these limits are strongly influenced by the preparation conditions.

For H:Sm ≈ 2, the hydrogen atoms enter the tetrahedral sites predominantly, but for $x > 0$ they also have to fill octahedral sites. Depending on the way in which the octahedral sites are occupied, two interesting phenomena are observed. When hydrogen atoms occupy these sites randomly, the proton self-diffusion process occurs more easily. However, if the occupation of the octahedral sites is not statistical, an ordered hydrogen sublattice and tetragonal metal lattice deformation are expected. We would like to report both effects here for the samarium hydrides.

2. Experimental details

The samples used in this study are the same as described in ref. 2. The accuracy of their atomic ratio H:Sm is ± 0.03. The continuous wave (Cw)

0925-8388/91/$3.50

nuclear magnetic resonance (NMR) experiment details are also in ref. 2. Debye X-ray diffraction patterns were used to obtain the structure and the lattice constant. A laboratory-made X-ray diffractometer (Fe Kα radiation, $\lambda = 1.93597$ Å) was used for this purpose [3]. It included a θ–2θ goniometer and a liquid nitrogen (or helium) cryostat at the bottom of which the sample was glued onto a cold copper finger.

3. Results and discussion

The proton Cw spectra obtained over a temperature range from about 78 K to 295 K indicated a lack of any changes for $SmH_{2.00}$ and a linewidth narrowing onset at about 250 K for $SmH_{2.12}$ (see Fig. 1). The temperature behaviour of the $SmH_{2.30}$ and $SmH_{2.40}$ spectra is more complicated. A single, narrow lorentzian-like line at room temperature broadens when the temperature is lowered, and near 250 K a composite system of broad and narrow resonance lines appears. Figure 1 shows the temperature dependence of the linewidth in the region where it could be determined with good precision. Below $T \approx 250$ K, the superposition of the two lines prevents further linewidth measurements.

The resonance absorption derivative for $SmH_{2.00}$ is shown in Fig. 2. Its shape can be well fitted by Abragam's proposed function [4]:

$$G(h) = \frac{1}{2ab(2\pi)^{1/2}} \int_{-b}^{b} \exp\left[\frac{-(h-x)^2}{2a^2}\right] dx \tag{1}$$

where $h = H - H_0$ and a and b are the parameters. An example of the fit to the measured derivative of the absorption resonance line is shown in Fig. 3. By using the following relation [4]:

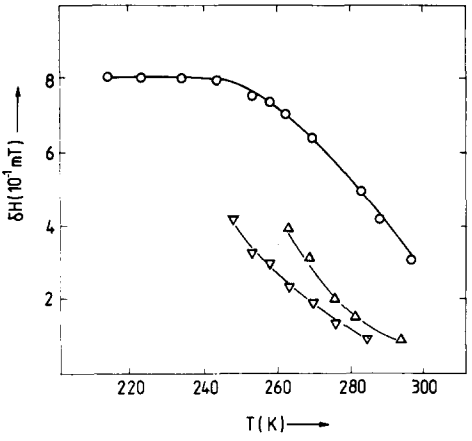

Fig. 1. The temperature dependence of the proton resonance linewidth in $SmH_{2.12}$ (○), $SmH_{2.30}$ (△) and $SmH_{2.40}$ (▽). Data are taken at a Larmor frequency of 15 MHz.

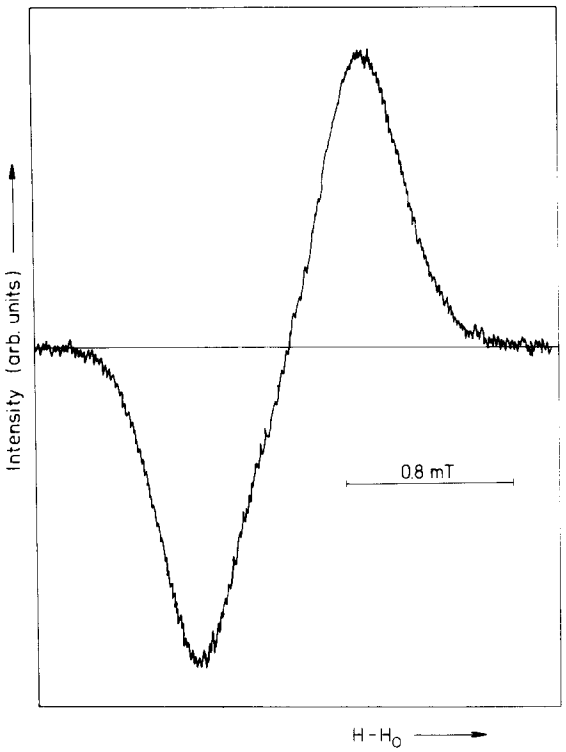

Fig. 2. An example of the absorption mode derivative spectrum of the ^1H resonance in $SmH_{2.00}$ at a resonance frequency of 5.96 MHz and $T = 78$ K.

$$m_2 = a^2 + \frac{b^2}{3}$$

$$m_4 = 3a^4 + 2a^2b^2 + \frac{b^4}{5} \tag{2}$$

the second (m_2) and fourth (m_4) moments can be estimated. They had to be corrected for finite modulation amplitude [5] and then values of $m_2 = 8.5 \pm 0.5 \times 10^{-2}$ mT^2 and $m_4 = 186 \pm 15 \times 10^{-4}$ mT^4 are obtained. Since the data were taken at relative low magnetic field (≈ 0.14 T), the demagnetization effects [6, 7] only influenced the spectra to a small extent. We estimate that their contribution to the moments is within experimental uncertainties. Experimentally obtained moments may be compared with calculated ones using the Van Vleck formula [8] and X-ray data for crystal lattice structure. The second and fourth moments derived for the CaF_2 type of structure are [9]:

$$m_2 = \frac{C_2 a_0^{-6}}{2\beta + \alpha} (115.6\ \alpha^2 + 2640\ \alpha\beta + 1075\ \beta^2)$$

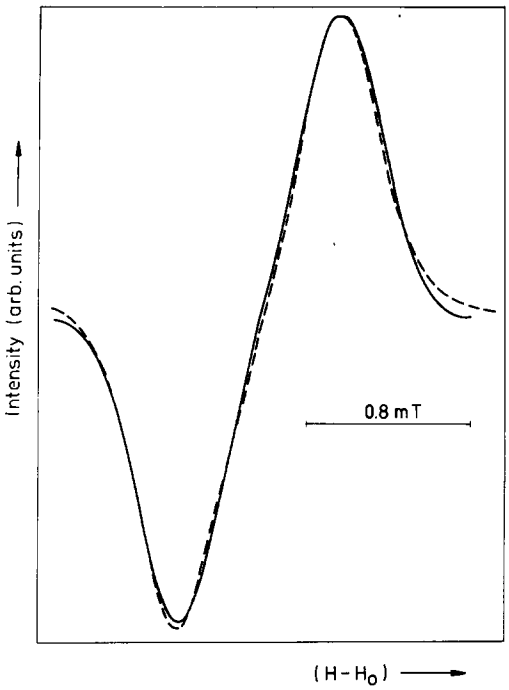

Fig. 3. Comparison of the absorption derivative ^{1}H NMR lines obtained from experiment (broken line) and from a least-squares fit to eqn. (1) (solid line). Here, the experimental recording presented in Fig. 2 is reproduced without noise for better illustration of the agreement between the two lines. The fitting parameters a and b are 0.19 mT and 0.383 mT respectively.

$$m_4 = \frac{C_4 a_0^{-12}}{2\beta+\alpha}(4.47\times10^6\beta^3+9.13\times10^4\alpha^3+7.29\times10^6\alpha^2\beta+2.18\times10^7\alpha\beta^2 + 3.53\times10^5\beta^2+5.39\times10^3\alpha^2+2.56\times10^6\alpha\beta) \quad (3)$$

$C_2 = 3.582\times10^{-6}(\mathrm{nm^6\ mT^2})$ $\quad C_4 = 3.96\times10^{-12}\ (\mathrm{nm^{12}\ mT^4})$

where α and β are the probabilities of occupancy in octahedral and tetrahedral sites respectively. The constants C_2 and C_4 were calculated for protons and the contribution of samarium nuclei moments has been neglected because of their low abundances and moments. The lattice constant $a_0 = 0.5358$ nm was taken from X-ray experiments. Assuming $\alpha = 0.03$ and $\beta = 0.985$, we obtained $m_2 = 8.5\times10^{-2}$ mT^2 and $m_4 = 188.5\times10^{-4}$ mT^4, values which agree with the above-mentioned experimental values. Earlier work [10] on proton NMR second moment analysis for LaH_2 gave $\alpha = 0.05$ and $\beta = 0.975$. Hence, in both cases the hydrogen atoms mostly occupy tetrahedral sites with only a few being located in octahedral sites. Also, in $SmH_{2.12}$ the lineshape of the ^{1}H NMR resonance at low temperature can be described using eqn. (1) and the moments thus obtained are $m_2 = 10.6\pm0.5\times10^{-2}$ mT^2 and $m_4 = 299\pm30\times10^{-4}$ mT^4. One then obtains very similar calculated values of $m_2 = 10.6\times10^{-2}$ mT^2 and $m_4 = 298\times10^{-4}$ mT^4 for $\alpha = 0.18$ and $\beta = 0.97$,

and $a_0 = 0.535$ nm. It again indicates a very large percentage of tetrahedral occupancy and an increased probability of octahedral site occupancy, necessary now to accommodate the larger number of hydrogen atoms (H:Sm = 2.12).

The proton linewidth in $SmH_{2.12}$, which is constant at low temperature, starts to narrow in the vicinity of 250 K (Fig. 1) owing to rapid thermally activated self-diffusion of the protons. In this case, the linewidth δH is related to the dipolar correlation time τ_d by the Kubo and Tomita [11] expression:

$$\tau_d = C_d(\delta H)^{-1} \tan\left[\frac{\pi}{2}\left(\frac{\delta H}{\delta H_0}\right)^2\right] \tag{4}$$

where for protons $C_d = 3.2 \times 10^{-6}$ (s mT), and the rigid-lattice (δH_0) and measured (δH) linewidths are given in milliTesla. Assuming, as customary, that:

$$\tau_d = \tau_0 \exp(E/kT) \tag{5}$$

then the activation energy E is determined from the plot of $\ln \tau_d$ *vs.* $1/T$. Before applying the above equations, one has to take into account the fact that the entire linewidth is not related to the dipolar interaction. There is a contribution from demagnetization effects [6, 7] caused by the paramagnetism of the samarium hydride sample. This contribution has been estimated from the temperature dependence of the magnetic susceptibility [7] and by determining the magnetic field dependence of the linewidths. Thus, the observed linewidths (Fig. 1) were corrected by subtracting the magnetic field broadening mentioned above. A least-squares fit of the data to eqns. (4) and (5) then yields $E = 36.8 \pm 3$ kJ mol^{-1} and $\tau_0 = 2 \times 10^{-11}$ s plus or minus a factor of 10.

The temperature behaviour of the proton spectra for $SmH_{2.30}$ and $SmH_{2.40}$ (Fig. 1) makes their interpretation more difficult than that of $SmH_{2.12}$. Although their linewidths indicate a self-diffusion of the protons, E and τ_0 cannot be determined because a two-line system is observed at low temperatures. A typical example of the superposition of these lines at $T = 238$ K is shown in Fig. 4 for $SmH_{2.40}$. This spectrum can be decomposed into two separate lines if one assumes that one of the lineshapes is described by eqn. (1) and the second one is lorentzian. The effect of the deconvolution is shown in Fig. 5. The parameters a and b of the first lineshape are 1.7×10^{-1} mT and 5.36×10^{-1} mT respectively. The linewidth of the lorentzian component δH_L (measured between maxima of the derivative of the absorption line) is equal to 0.38 mT. The contribution of the lorentzian line to the whole intensity of the spectrum is estimated to be 0.58 (see Appendix A). At a still lower temperature ($T = 78$ K), the moments of the broad line increase by about 15%, δH_L is ≈ 0.48 mT and the contribution of the lorentzian line to the total intensity remains the same.

A similar behaviour is exhibited by the spectra of the $SmH_{2.30}$ sample. However, in this case, about 0.4 of the total intensity (at $T = 78$ K) can be described by the lorentzian lineshape, and the moments of the second line are smaller than that of $SmH_{2.40}$.

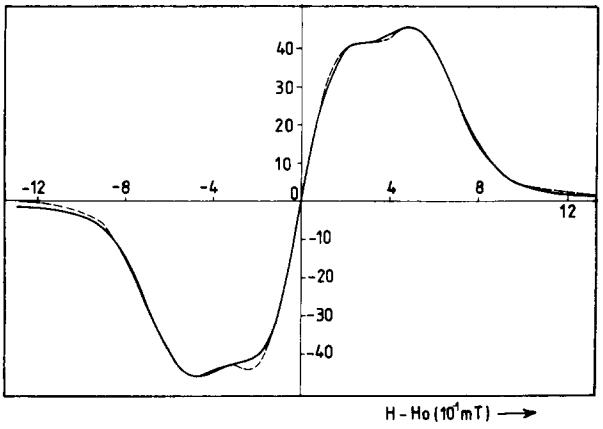

Fig. 4. Comparison of the measured absorption derivative ^{1}H NMR spectrum for $SmH_{2.40}$ with that obtained as a result of superposition of the two lines shown in Fig. 5 (solid line). The signal to noise ratio for the experimental spectrum (broken line) was similar to that shown in Fig. 2.

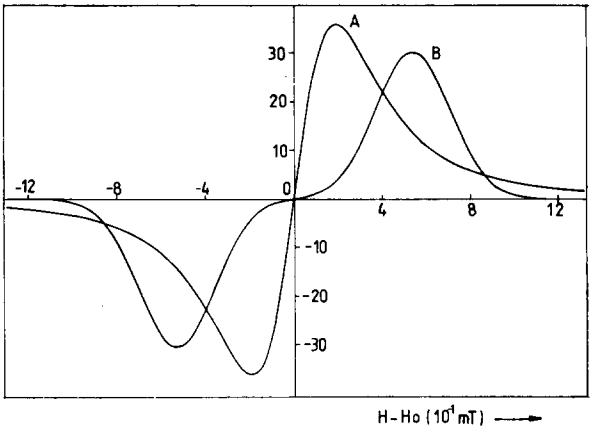

Fig. 5. The two resonance lines A and B resulting from the decomposition of the spectrum shown in Fig. 4. A is lorentzian in shape with $\delta H_L = 0.38$ mT whilst B is described by eqn. (1) with $a = 0.17$ mT and $b = 0.536$ mT.

The change from the one-line spectrum to the more complicated one was reported for ^{2}D NMR in LaD_{2+x} deuterides [12]. One narrow and two broad resonances were observed below 240 K for $2.28 < x < 2.48$. They have been attributed to the fact that deuterium atoms experienced different crystalline electric field gradients in the ordered deuterium sublattice. For SmH_{2+x} it is difficult to apply the same argument since protons are insensitive to these gradients. One possible explanation of the two-line system in $SmH_{2.30}$ and $SmH_{2.40}$ is to assume that below about 250 K the two phases might coexist. One of them may have an ordered structure on the hydrogen sublattice (broad line), whilst in the other one the hydrogen atoms are still relatively

mobile (lorentzian line). The ordering would probably lead to a restriction of the proton diffusion as well as inducing a cubic–tetragonal transformation of the f.c.c. lattice of the samarium ions.

In fact, such a lattice deformation has been observed by us for a $SmH_{2.30}$ sample. At room temperature we observed that for the $SmH_{2.30}$ sample the X-ray pattern is characteristic for the f.c.c. lattice with a lattice parameter $a_0 = 0.5365$ nm. However, when the temperature was lowered, a decrease of a_0 and an asymmetric broadening of the reflections at large angles were detected. In Fig. 6, a typical example of the diffraction line in the vicinity of $\theta = 70°$ is shown for $T = 171$ K. This reflection arises from (333), (511) and (115) indices. When tetragonal deformation takes place, the (333) line remains unchanged but the (511) and (115) lines are subject to splitting. The lattice parameters and c/a ratio deduced from our X-ray studies for $T = 98$ K are $a_0 = 0.5344$ nm and $c_0 = 0.5362$ ($c{:}a = 1.003$). For comparison, Knappe *et al.* [13] reported very similar values of $a_0 = 0.5343$ nm and $c_0 = 5365$ nm ($c{:}a = 1.004$) obtained at room temperature for $SmH_{2.33}$. However, in our sample the tetragonal deformation occurs at lower temperatures.

The X-ray data taken for $SmH_{2.12}$ indicate that it remains cubic between $T = 12$ K and $T = 293$ K. The result is in agreement with the conclusions drawn from both our ^1H NMR data and electrical resistivity measurements reported by Vajda *et al.* [14, 15]. However, the situation is more complicated for the $SmH_{2.40}$ sample, where we did not observe clear evidence of tetragonal deformation of the metal lattice. Instead of this, an increase in the width:height ratio for the $\theta = 70°$ reflection was observed between 112 K and 12 K. Probably the simplest explanation of that fact is to assume that the tetragonal deformation in $SmH_{2.40}$ is smaller than in $SmH_{2.30}$. This is prompted by the X-ray data in the LaH_{2+x} [16] and CeH_{2+x} [17] systems, where a small tetragonal deformation of the crystal lattice was also observed. In particular, it was found that the $c{:}a$ ratio for H:Ln of about 2.40 is smaller than that

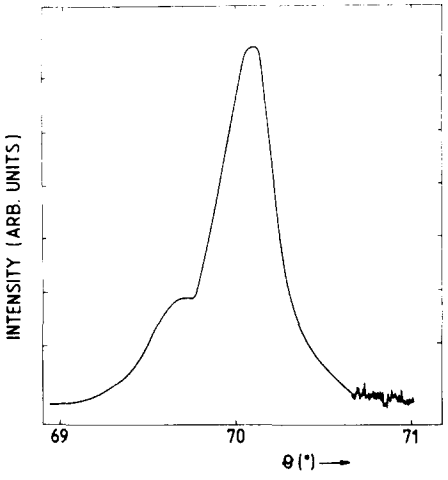

Fig. 6. X-ray diffraction line of $SmH_{2.30}$ at about $\theta = 70°$ taken at $T = 171$ K.

for the other hydrogen concentrations where a tetragonal deformation was detected. Finally, let us mention the recent paper by Daou *et al.* [18] on X-ray measurements in SmH_{2+x}. Although they do not report observation of a tetragonal phase, anomalies in the thermal expansion coefficients for $x = 0.26$ and $x = 0.45$ were seen. In summary, the present investigation of SmH_{2+x} shows that for $x = 0$ and $x = 0.12$ the samarium hydrides display properties similar to those of LaH_{2+x} [10]. However, the results for $x = 0.30$ and $x = 0.40$ indicate a phase transition in the vicinity of $T \approx 250$ K which is most probably owing to the ordering of the hydrogen sublattice.

Acknowledgment

O.J.Ż is grateful to the CNRS–PAN exchange program for partial support of this work.

References

1 O. Greis, P. Knappe and H. Mueller, *J. Solid. State Chem.*, *39* (1981) 49.
2 O. J. Żogał, M. Drulis and S. Idziak, *Z. Phys. Chem. N.F.*, *163* (1989) 303.
3 M. Barberon, *Doctoral Thesis, CNRS No. 702*, Paris, 1973.
4 A. Abragam, *The Principles of Nuclear Magnetism*, Clarendon, Oxford, 1961, p. 120.
5 E. R. Andrew, *Phys. Rev.*, *91* (1953) 425.
6 L. E. Drain, *Proc. Phys. Soc. (London)*, *80* (1962) 1380.
7 O. J. Żogał, *Phys. Status Solidi B*, *117* (1983) 717.
8 J. H. Van Vleck, *Phys. Rev.*, *74* (1948) 1168.
9 B. Staliński, C. K. Coogan and H. S. Gutowsky, *J. Chem. Phys.*, *34* (1961) 1191.
B. Nowak and O. J. Żogał, unpublished data, 1983.
10 D. S. Schreiber and R. M. Cotts, *Phys. Rev.*, *131* (1963) 1118.
11 R. Kubo and K. Tomita, *J. Phys. Soc. Jpn.*, *9* (1954) 888.
12 D. G. de Groot, R. G. Barnes, B. J. Beaudry and D. R. Torgeson, *J. Less-Common Met.*, *73* (1980) 233.
13 P. Knappe, H. Mueller and H. W. Mayer, *J. Less-Common Met.*, *95* (1985) 323.
14 P. Vajda, J. N. Daou and J. P. Burger, *Phys. Rev. B*, *40* (1989) 500.
15 P. Vajda, J. N. Daou and J. P. Burger, *Z. Phys. Chem. N.F.*, *163* (1989) 637.
16 E. Boroch, K. Conder, Cai Ru-Xiu and E. Kaldis, *J. Less-Common Met.*, *156* (1989) 259.
17 E. Kaldis, E. Boroch and M. Tellefsen, *J. Less-Common Met.*, *129* (1987) 57.
18 J. N. Daou, P. Vajda and J. P. Burger, *Solid State Commun.*, *71* (1989) 1145.

Appendix A

When resonance lines are recorded as first derivatives, their intensities can be determined either by double integration or by using appropriate formulae. First integration gives the absorption, and the result of such a procedure for the derivatives from Fig. 4 is shown in Fig. A1. The area (P) under lines A and B is a measure of their intensities. In particular, $I_A = P_A/(P_A + P_B)$ is the relative intensity of line A (here the lorentzian one).

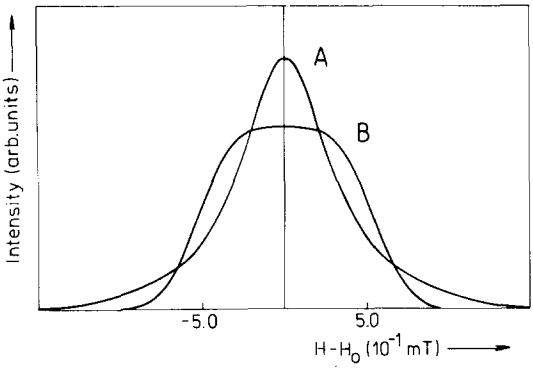

Fig. A1. The absorption lines A and B obtained by integration of their first derivatives as shown in Fig. 5.

Another method can be applied when the lineshape functions are known. In our case, we have:

$$P_A = (2\pi/3^{1/2})(\delta H_L)^2 g'_{max} \tag{A1}$$

$$P_B \simeq 2ab(2\pi)^{1/2} g'_{max} \tag{A2}$$

where g'_{max} is the maximum value of the first derivative and the formulae are valid for the lorentzian and eqn. (1) lineshape functions respectively. In the latter, the approximation is very good for $b/2a > 1$.